

Malignant Extrarenal Rhabdoid Tumor in Adults: Three Case Reports Originating from the Ileum, Adrenal Gland and Uterus¹

성인의 회장, 부신, 자궁에서 생긴 악성 신외성 횡문근양 종양: 증례 보고¹

Euddeum Shim, MD¹, Suk Keu Yeom, MD¹, Jun Won Um, MD², Jin Hee Kim, MD³,
Seung Hwa Lee, MD¹, Sang Hoon Cha, MD¹, Jung-Woo Choi, MD⁴

Departments of ¹Radiology, ²Colorectal Surgery, ⁴Pathology, Ansan Hospital, Korea University College of Medicine, Ansan, Korea

³Department of Radiology, Asan Medical Center, University of Ulsan College of Medicine, Seoul, Korea

Malignant extrarenal rhabdoid tumor (MERT) is a very aggressive tumor that is extremely rare in adults. Herein, we introduce three cases of MERT in adults that originated in the ileum, adrenal gland, and uterine endometrium. The MERTs in the ileum and adrenal gland showed non-aggressive features and a good prognosis, while the MERT in the uterine presented with aggressive features and distant metastasis.

Index terms

Rhabdoid Tumor
Ileum
Uterus
Adrenal Gland
Computed Tomography
Fluoroscopy

INTRODUCTION

It has been known that malignant rhabdoid tumor, which was first reported by Beckwith and Palmor in 1978, is a very aggressive renal tumor in infants and children (1). It is a rare tumor, accounting for less than 2% of renal malignancies in children and even fewer in adults. However, it has been reported that the tumor can originate in organs other than the kidney, including the central nervous system, orbit, lacrimal gland, uterus, skin, and gastrointestinal tract. These tumors are referred to as malignant extrarenal rhabdoid tumor (MERT). The mean age of the patients with MERT is about 12 months, but ages range from 3 weeks to 70 years with no demonstrable gender predication. MERT shows same features as malignant rhabdoid tumor of the kidney, in microscopic studies of pathology, genetics, and prognosis (1).

MERT is usually aggressive by the time of diagnosis, resulting in poor prognosis. We present three cases of MERT in adults

originating from the ileum, adrenal gland, and uterus.

CASE REPORT

Case 1

A 52-year-old woman was admitted to an emergency department after cramping, abdominal pain, and vomiting for one day. The contrast-enhanced CT scan showed a solid mass in the distal ileum (Fig. 1A). The mass was 2.3 cm in size with good contrast-enhancement. It appeared as an intra-luminal protrusion into the bowel lumen and presented with desmoplastic reaction at the mesentery. Our initial assessment found the signs similar to adenocarcinoma of the small bowel, rather than a submucosal tumor such as a neuroendocrine tumor, gastrointestinal stromal tumor, or lymphoma. There was no mechanical obstruction of the small bowel. The symptoms improved with conservative management including hydration and analgesics, but recurred on the fifth day of hospitalization. The patient underwent ene-

Received January 28, 2014; Accepted May 13, 2014

Corresponding author: Suk Keu Yeom, MD
Department of Radiology, Ansan Hospital, Korea
University College of Medicine, 123 Jeokgeum-ro,
Danwon-gu, Ansan 425-707, Korea.
Tel. 82-31-412-5228 Fax. 82-31-412-5224
E-mail: pagoda20@gmail.com

This is an Open Access article distributed under the terms of the Creative Commons Attribution Non-Commercial License (<http://creativecommons.org/licenses/by-nc/3.0>) which permits unrestricted non-commercial use, distribution, and reproduction in any medium, provided the original work is properly cited.

ma with water-soluble contrast medium (Gastrografin, Bayer Healthcare, Berlin, Germany) and showed an ileocolic-type intussusception (Fig. 1B, C). The intussusceptum moved proximally with the pressure of the enema, revealing a tumor originating in the distal ileum, which was not completely resolved with the enema. Therefore, emergent laparoscopic exploration was conducted, followed by a radical resection from the distal ileum to the hepatic flexure of the colon with extended lymph node dissection. The pathologic examination revealed absence of metastasis in a total of 28 dissected regional lymph nodes.

The tumor was 3.5 cm in size and was located 20 cm proximal to the ileocecal valve. The mass was polypoid at the mucosal sur-

face and invaded the muscularis propria (Fig. 1D-F). The lymphatic tumor emboli were noted on microscopic examination, which were composed of polygonal and loosely cohesive cells. The individual cells had large, eccentric nuclei with homogeneously eosinophilic cytoplasm and intra-cytoplasmic inclusions reminiscent of malignant rhabdoid tumor cells. The tumors were positive for vimentin and CD56, and negative for CAM5.2, cytokeratin, HMB45, synaptophysin, Alcian blue-pH2.5, CD34, and D2-40.

The patient recovered without any postoperative complications, and underwent follow-up imaging studies including contrast-enhanced abdominal-pelvic CT and contrast-enhanced

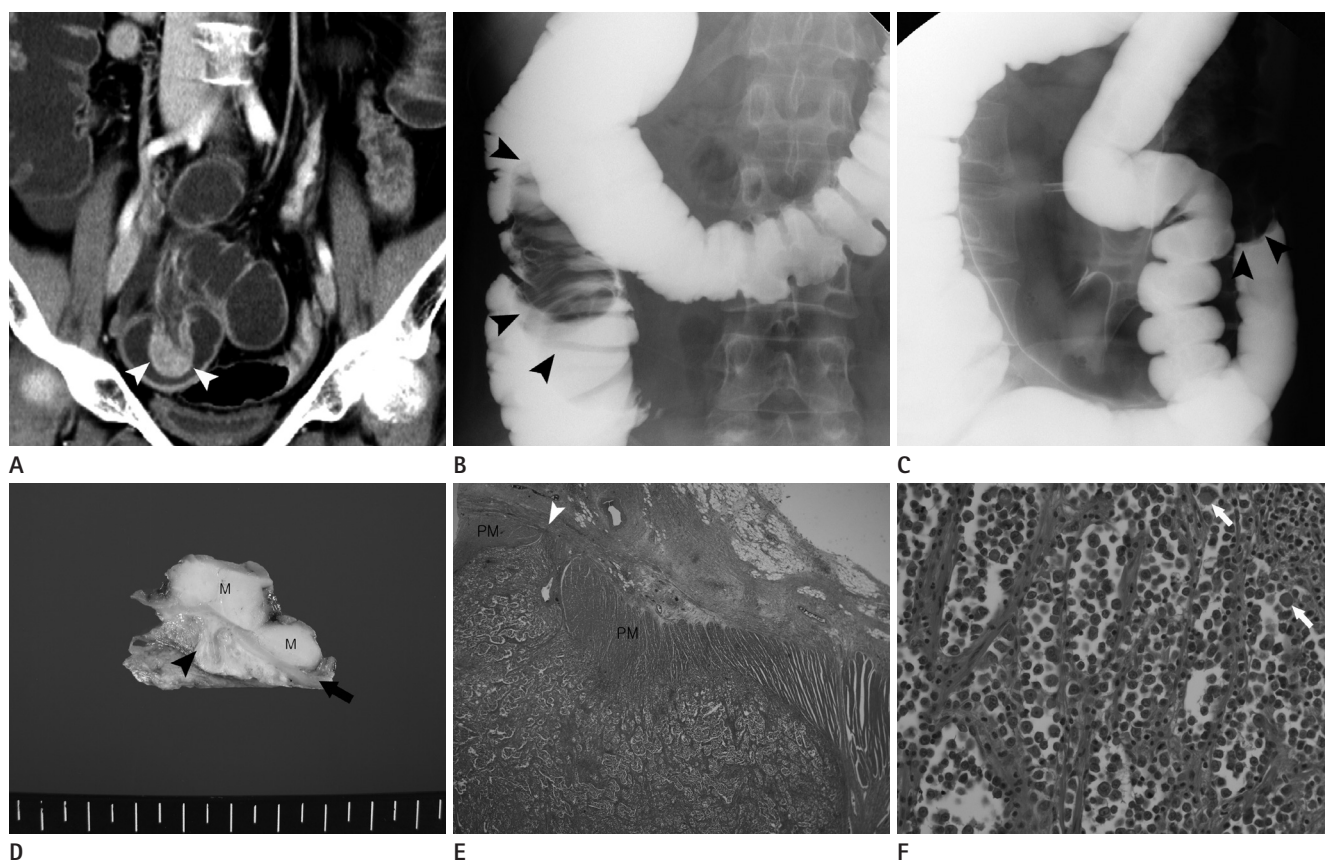


Fig. 1. A 52-year-old woman suffered from cramping abdominal pain.

- A.** A 70-second-delayed contrast-enhanced coronal CT scan shows a well-enhanced mass (arrowheads) in the distal ileum. The mass has an intraluminal protruding appearance and no luminal obstruction.
- B.** On 5 days from initial study, contrast enema with water-soluble contrast medium (Gastrografin) is performed due to recurred pain. It shows an ileocolic type intussusception (arrowheads).
- C.** The intussusception (arrowheads) is moved proximally to the distal ileum with the pressure of the enema, but not completely resolved.
- D.** The mass (M) is protruding at the mucosal surface, and the cut surface of the tumor is pale yellow, invading the muscular layer (arrow) and sparing the adventitia (arrowhead) macroscopically.
- E.** In a low-power field-microscopic photograph (H&E stain, $\times 40$), the tumor penetrates the entire proper muscle (PM) layer (arrowhead), and lymphatic tumor emboli are noted.
- F.** In a high-power field-microscopic photograph (H&E stain, $\times 400$), the tumor is composed of polygonal and loosely cohesive cells. The cells show large, eccentric nuclei, homogenous eosinophilic cytoplasm, and intra-cytoplasmic inclusions (arrows), concordant with rhabdoid cells.

chest CT at 2, 6, and 12 months after the operation, and positron emission tomography-CT at 2 months after the operation. No tumor recurrence or distant metastasis was detected.

Case 2

A 63-year-old man visited the emergency department due to abdominal pain that had been present for 3 months. The contrast-enhanced CT scan revealed a 10-cm, well-defined, round-shaped mass in the right upper abdominal cavity. The mass presented with relatively low attenuation compared to the liver on the pre-contrast-enhanced CT scan and poor enhancement on the 1-, 2-, and 15-minute delayed phases of the contrast-enhanced scans. The mass was positioned at a blunt angle to the right adrenal gland, suggesting that the origin was the adrenal gland (Fig. 2A, B). There was no lymphadenopathy or distant metastasis on imaging studies. The Iodine-123 MIBG scan revealed a 'cold defect', eliminating the possibility of functional pheochromocytoma.

A laparoscopic mass excision was performed. The tumor was 13 × 12 × 8 cm on gross specimen. There were no lymphovascular emboli or perineural invasion. The tumor showed hemorrhagic and myxoid foci (Fig. 2C). The tumor was composed of sheets of polygonal cells containing eosinophilic cytoplasmic inclusion. Immunohistochemical staining of the tumor was positive for cytokeratin and negative for SMA, CD10, epithelial membrane antigen (EMA), HNB45, CD34, vimentin, inhibin, S-100 protein, desmin, and chromogranin.

The patient recovered without complications and presented

no tumor recurrence or distant metastasis on imaging studies for over 2 years after the operation.

Case 3

A 58-year-old woman was admitted to the hospital due to vaginal spotting that had been present for 5 months. A palpable, hard mass was detected by physical examination in the low abdominal cavity. The contrast-enhanced pelvis MRI showed a 10-cm mass in the uterine endometrial cavity. The mass presented with heterogeneous high-signal intensity on T2-weighted images and heterogeneous low-signal intensity on T1-weighted images. The mass showed poor contrast enhancement and multiple T1 high-signal and T2 low-signal intensity foci in the central portion, representing hemorrhage on MR images (Fig. 3A-C). Several enlarged lymph nodes were detected along both internal iliac chains. In addition, multiple uterine leiomyomas appeared as low-signal intensity on T1- and T2-weighted images. The patient underwent total abdominal hysterectomy, left salpingo-oophorectomy, and radical lymph node dissection, including pelvic and paraaortic lymph nodes.

The tumor was 11.5 cm in size and originated from the uterine endometrium. The mass involved more than 50% of the depth of the myometrial layer. Seven metastatic lymph nodes were diagnosed in a total of 51 lymph nodes.

On microscopic images, typical rhabdoid morphology was noted. On immunohistochemical stain study, CD99, integrase interactor 1 (*INI1*), and vimentin were positive and myogenin, cytokeratin, and epithelial membrane antigen were negative.



Fig. 2. A 63-year-old man presenting a right adrenal gland mass.

A. A pre-enhanced CT scan shows well-defined, round-shaped, low attenuating mass in the right upper abdominal cavity.

B. An 120-second-delayed contrast-enhanced CT scan shows poor enhancement of the mass. The mass is positioned at a blunt angle to the right adrenal gland (arrowheads).

C. The cut surface of the tumor is pinkish tan and soft with hemorrhagic and myxoid foci.

Multiple pelvic tumors and retroperitoneal lymphadenopathy were detected on the follow-up CT scan performed 3 months after the operation, suggesting a tumor recurrence (Fig. 3D, E). The patient expired 9 months after the operation.

DISCUSSION

Malignant rhabdoid tumor was first described as a sarcomatous variant of Wilm's tumor (1). However, because of the absence of ultrastructural or immunohistochemical evidence of myogenic differentiation, the term "rhabdoid tumor" was adopted, based on the rod-like shape of the tumor cells. The rhabdoid cells typically present with a large polygonal appearance with juxtannuclear, globular, and eosinophilic inclusions in the cytoplasm and vesicular nuclei that often contain a single prominent nucleolus. The histologic diagnosis of MERT is confirmed by identifying rhabdoid cells in the tumor. The architecture of a tumor usually consists of a solid pattern, but it can also have tra-

becular, pseudo-alveolar, and myxoid patterns (2).

The histologic origin of MERT is unclear. The term 'malignant rhabdoid tumor' has been used to describe a heterogeneous group of neoplasms that have distinct so-called "rhabdoid" cytologic features in common. However, for malignant rhabdoid tumors, 70% of the primary tumors share a similar mutation or loss of the tumor-suppressor gene SWI/SNF-related, matrix-associated, actin-dependent regulator of chromatin, subfamily b, member 1 (*SMARCB1*), also known as *INI1* on chromosome 22q11.2. This unique gene makes this tumor a distinct entity (3). It has also been reported that rhabdoid tumors can arise within neural stem cells during a critical developmental period, in which a loss of *SMARCB1* directly results in repression of neural development (4).

There is a controversy regarding the development of malignant rhabdoid tumors, with two prominent hypotheses: de novo from non-neoplastic cells or through tumor progression from other types of neoplasm. Therefore, it is suggested that other

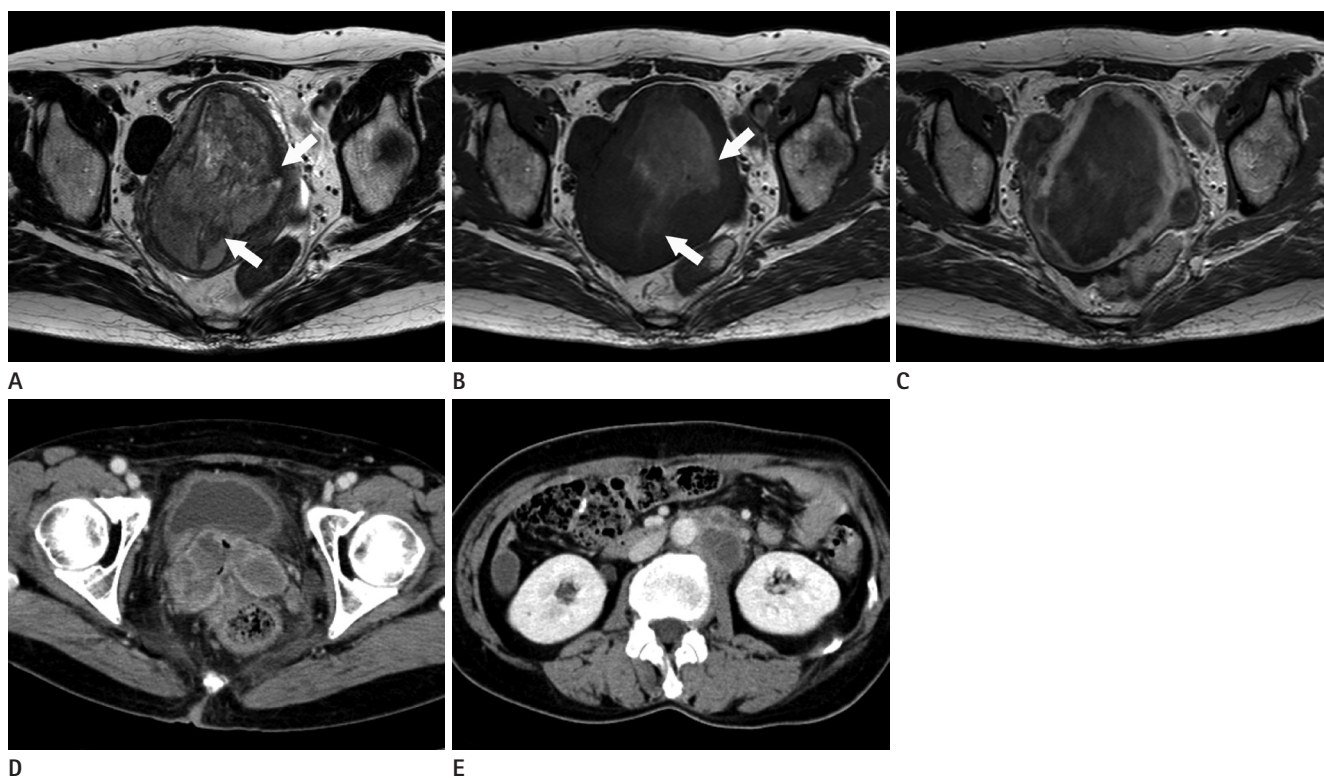


Fig. 3. A 58-year-old woman complaining vaginal spotting.

A, B. The uterine endometrial mass presents with heterogeneous high-signal intensity on T2-weighted image (**A**) and heterogeneous low-signal intensity on T1-weighted image (**B**). Multiple T2 low-signal and T1 high-signal intensity foci in the mass, representing hemorrhage (arrows).

C. Contrast-enhanced T1-weighted MR image shows poor enhancement of the mass.

D, E. Contrast-enhanced CT scan images performed 3 months after the operation show multiple pelvic tumors and retroperitoneal lymphadenopathy.

non-rhabdoid tumor components are found in the tumor, and may be referred to as composite malignant rhabdoid tumors. This focal “rhabdoid phenotype” may be present in various mesenchymal and epithelial malignancies including squamous carcinoma, malignant melanoma, and synovial sarcoma. It has been accepted that the rhabdoid phenotype is usually associated with worst prognosis (5).

Because immunohistochemistry is available in clinical practice more often than a molecular gene assay, immunostaining with *INI1/BAF47* antibody can be used to confirm malignant rhabdoid tumor, instead of analysis of the *SMARCB1/INI1* genes. Malignant rhabdoid tumor shows polyphenotypic immunohistochemical profiles and positive results for a variety of antigens including epithelial, mesenchymal, and neural antigens. Fanburg-Smith et al. (6) evaluated the immunohistochemical features of 28 cases of rhabdoid tumors and reported that rhabdoid tumors were mainly positive for vimentin, which is a type III intermediate filament protein that is expressed in mesenchymal cells and used as a sarcoma tumor marker to identify the mesenchyme. The EMA and cytokeratin are found in the intra-cytoplasmic cytoskeleton of epithelial tissue and have been used as tumor markers of epithelial origin; they appear to be the next most frequently expressed markers. Some malignant rhabdoid tumors may be positive for CAM5.2, MSA, CEA, SMA, CD99, synaptophysin, or neuron-specific enolase including CD57 (Leu-7), NSE, and focal S100 protein (6).

To our knowledge, a primary malignant rhabdoid tumor in the gastrointestinal (GI) tract is extremely rare. A total of 28 cases of malignant rhabdoid tumor involving the GI tract have been reported, and the stomach is the most frequently involved (8 cases), followed by 10 cases of small bowel (1 duodenum, 7 jejunum, and 1 ileum), 7 cases of colon, and 3 cases of esophagus (7). The patients with MERT in the GI tract are older (mean, 67.9 years; range, 52–84 years) than patients who have the same tumor elsewhere. Furthermore, men are 3.6 times more likely than women to develop GI tract MERT. However, none or only a slight male predilection has been generally reported for MERT elsewhere. The diameter of the primary tumor exceeded 5 cm in most cases. The most common sites of metastasis were the liver, adrenal glands, and regional lymph nodes. The prognosis of MERT in the GI tract is very poor, and the median rate of survival is approximately 5.5 months (8).

Only one case of primary adrenal gland MERT has been reported, and the patient was a 3-year-old boy (9). Both tumors showed no invasion into the adjacent organs, contrary to the aggressive imaging features of MERT originating elsewhere, despite the huge size of over 10 cm in diameter. Our case had results with positivity for cytokeratin stain, in accordance with the previous case which had positivity for cytokeratin and EMA by immunohistochemistry.

MERT arising from the female genitalia has been reported in 12 cases of the vulva, 5 cases of the uterus (except mixed form), and one case of the ovary. The ages at the onset of the diseases ranged from 18 to 71 years (mean age, 38 years). It was reported that 6 surgically treated female genitalia MERT patients had lived for more than 30 months. Female genitalia MERT showed positive staining for vimentin, cytokeratin, and EMA.

There are no known pathognomic imaging findings for MERT. The tumor is usually large and presents with parenchymal heterogeneity without capsulation, on various imaging modalities including ultrasonography, computed tomography, and MRI; this is due to frequent intra-tumoral necrosis and hemorrhage, which suggests a rapid tumor growth (1).

Upon diagnosis, most tumors show extensive aggressive features with invasion into the adjacent organs or distant metastasis, including the liver, retroperitoneal space, pancreas, adrenal gland, and urinary bladder.

Our case of GI tract MERT was small in size (less than 3 cm) with no distant metastases, probably due to early symptoms such as bowel obstruction. In this case, the tumor showed a homogeneous enhancement pattern. It was reported in another study that MERT detected early in the subcutaneous layer of the abdominal wall was small in size with homogeneous enhancement (10). In both cases, a complete excision of the tumor was achieved and the prognosis was excellent.

The best treatment for MERT is the complete surgical resection, and there is no established adjuvant therapy. The post-operative chemotherapy and radiation therapy are usually attempted in most MERT patients with aggressive features, using an alkylating agent such as doxorubicin. However, the benefits of these adjuvant therapies are not clear.

In summary, MERT is an extremely rare tumor in adults, with aggressive features and poor prognosis. They usually present as large heterogeneous tumors on imaging studies. However, they

can also be small homogeneously enhanced tumors with excellent prognosis, if detected early enough.

REFERENCES

1. Abdullah A, Patel Y, Lewis TJ, Elsamaloty H, Strobel S. Extrarenal malignant rhabdoid tumors: radiologic findings with histopathologic correlation. *Cancer Imaging* 2010;10:97-101
2. Haas JE, Palmer NF, Weinberg AG, Beckwith JB. Ultrastructure of malignant rhabdoid tumor of the kidney. A distinctive renal tumor of children. *Hum Pathol* 1981;12:646-657
3. Biegel JA, Kalpana G, Knudsen ES, Packer RJ, Roberts CW, Thiele CJ, et al. The role of INI1 and the SWI/SNF complex in the development of rhabdoid tumors: meeting summary from the workshop on childhood atypical teratoid/rhabdoid tumors. *Cancer Res* 2002;62:323-328
4. Gadd S, Sredni ST, Huang CC, Perlman EJ; Renal Tumor Committee of the Children's Oncology Group. Rhabdoid tumor: gene expression clues to pathogenesis and potential therapeutic targets. *Lab Invest* 2010;90:724-738
5. Ogino S, Ro TY, Redline RW. Malignant rhabdoid tumor: A phenotype? An entity?--A controversy revisited. *Adv Anat Pathol* 2000;7:181-190
6. Fanburg-Smith JC, Hengge M, Hengge UR, Smith JS Jr, Miettinen M. Extrarenal rhabdoid tumors of soft tissue: a clinicopathologic and immunohistochemical study of 18 cases. *Ann Diagn Pathol* 1998;2:351-362
7. Tóth L, Nemes Z, Gomba S, Asztalos L, Molnár C, András C, et al. Primary rhabdoid cancer of the ileum: a case report and review of the literature. *Pathol Res Pract* 2010;206:110-115
8. Salamanca J, Nevado M, Martínez-González MA, Pérez-Espejo G, Pinedo F. Undifferentiated carcinoma of the jejunum with extensive rhabdoid features. Case report and review of the literature. *APMIS* 2008;116:941-946
9. Yaris N, Cobanoglu U, Dilber E, Ahmetoğlu A, Saruhan H, Okten A. Malignant rhabdoid tumor of adrenal gland. *Med Pediatr Oncol* 2002;39:128-131
10. Horazdovsky R, Manivel JC, Cheng EY. Successful salvage and long-term survival after recurrent malignant rhabdoid tumor. *Sarcoma* 2007;2007:53549

성인의 회장, 부신, 자궁에서 생긴 악성 신외성 횡문근양 종양: 증례 보고¹

심으뜸¹ · 염석규¹ · 엄준원² · 김진희³ · 이승화¹ · 차상훈¹ · 최정우⁴

악성 횡문근양 종양은 매우 예후가 안좋은 종양으로서 성인에서 발생하는 경우는 드물다. 우리는 각기 다른 세 사람에게서 생겼던 회장과 부신, 그리고 자궁에서 발생한 악성 횡문근양 종양을 경험하여 그 영상 소견을 소개하고자 한다. 회장과 부신에서 생겼던 종양은 덜 침습적이고 좋은 예후를 보였던 반면 자궁에서 생겼던 종양은 매우 침습적인 모습과 원격전이를 동반한 모습이었다.

고려대학교 의과대학 안산병원 ¹영상의학과, ²대장항문외과, ⁴병리과, ³울산대학교 의과대학 서울아산병원 영상의학과